Int j simul model 19 (2020) 2, 303-312
ISSN 1726-4529 Original scientific paper

# MATHEMATICAL MODELLING AND SIMULATION OF A NOVEL HYDRAULIC VARIABLE VALVE TIMING SYSTEM

Xu, Y. L.[*,#]; Nie, H. W.[**]; Zhao, H. L.[***] & Liu, J.[*]
[*] School of Mechanical Engineering, Guiyang University, Guiyang 550005, China
[**] Guizhou Communications Polytechnic, Guiyang 551400, China
[***] Guizhou Minzu University, Guiyang 550025, China
E-Mail: hlzhao@gzmu.edu.cn ([#] Corresponding author)

**Abstract**
This paper explores deep into the mathematical modelling and simulation of a novel hydraulic variable valve timing (VVT) system. Considering the structure of the target system and the influencing factors of valve motions, the mathematical models were established for oil compressibility, pressure loss of pipeline, oil cylinder of cam, oil cylinder and buffer mechanism of the valve, oil cylinder of regulator, and the oil supply. On this basis, a simulation model was established on AMESim to analyse and optimize the motion parameters of the hydraulic VVT system. Finally, the simulated results were compared with early test results. The comparison shows that the simulated results are in good agreement with the test results, indicating that our simulation model is highly reliable. The research findings lay a solid basis for parameter analysis and optimization of VVT systems.
(Received in October 2019, accepted in February 2020. This paper was with the authors 3 months for 1 revision.)

**Key Words:** Hydraulic Variable Valve Timing (VVT) System, Mathematical Modelling, Simulation, AMESim

## 1. INTRODUCTION

In variable valve timing (VVT), the valve is adjusted reasonably according to the change of engine operations, aiming to improve the engine power, reduce fuel consumption and slash exhaust emissions [1-5]. Many VVT systems, especially those of variable camshaft timing (VCT), have been widely applied.

The most representative VVT systems include Toyota's VVT-i (variable valve timing with intelligence) and Ford's VCT (variable camshaft timing). But neither of them can change the duration angle and maximum lift according to engine speed [6, 7]. BWM's Valvetronic and VANOS (VAriable NOckenwellen Steuerung) systems can continuously regulate the valve timing and maximum lift, and fully satisfy the requirements on valve timing. However, the systems are too costly and complex in structure [8]. Honda's VTEC (variable valve timing & lift electronic control), Audi's AVS (Audi valve-lift system) and MIVEC (Mitsubishi innovative valve timing electronic control system) rely on a variable cam mechanism containing two or three cams. The mechanism can only realize optimal valve timing at two or three engine speeds, failing to achieve continuous VVT at different engine speeds. Fiat's 3D cam mechanism can regulate valve timing and maximum lift by changing the contact position between the cam and the follower. The mechanism has not been effectively applied, because the point contact between the two components is prone to serious wear. In addition, the single spring electro-hydraulic VVT system developed by Lotus can adjust the valve timing and maximum lift in the light of engine operations. Besides high cost and complex structure, the said system controls each valve separately and requires fast electromagnetic response [9-12].

The modelling of hydraulic VVT system has attracted much attention from the academia. Khajepour et al. put forward a novel hydraulic VVT system, built a mathematical model of the system, and relied on the model to analyse the repeatability and reliability of valve adjustment [13-16]. Wong et al. simulated an electro-hydraulic fully VVT system on

MATLAB, and examined the features of valve adjustment [17, 18]. Xie et al. developed a hydraulic VVT system, and established differential equations to explore the pressure fluctuations, cam design and valve motions of the system [19]. Many other scholars have also probed deep into the modelling of hydraulic VVT system [20-22].

The significance of mathematical modelling and simulation of hydraulic VVT system has been widely recognized: the established models and simulation results provide insights into valve motions, and facilitates the optimization of system structure, laying a solid basis for improving the theories and performance of hydraulic VVT system [23-25].

In this paper, mathematical modelling and simulation are performed on a cam-driven hydraulic volume-adjustable continuous VVT system. Compared with existing VVT systems, the target system, despite its simple structure, can adjust the valve phase and lift continuously, thereby improving engine performance. According to early tests and analyses, the valve motions in the system are under the complex impacts from multiple factors, including oil compression, pressure fluctuations, adjustment performance and seating features.

The remainder of this paper is organized as follows: Section 2 introduces the composition and working principle of the target VVT system; Sections 3 and 4 establish mathematical and simulation models of the said system, respectively; Section 5 compares the simulation results with test results; Section 6 puts forward the conclusions.

## 2. HYDRAULIC VVT SYSTEM

As shown in Fig. 1, the target hydraulic VVT system mainly consists of a cam assembly, a valve assembly, a regulator assembly, a seating snubber, and an oil supply. During the system operation, the camshaft drives the oil cylinder of cam; the driving force is hydraulically transmitted to drive the oil cylinder of valve, which then kicks off valve motions. The working principle of the target hydraulic VVT system is given below Fig. 1.

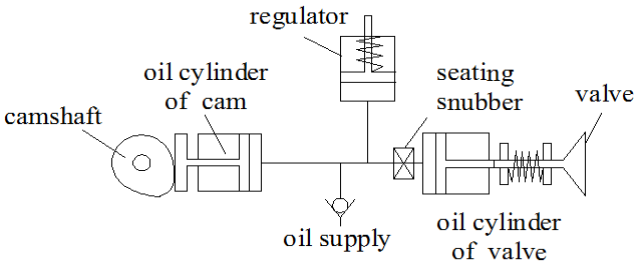


Figure 1: Structure of the target hydraulic VVT system.

When the cam is on the base circle, the plunger of the regulator lies at the very front of the oil cylinder. At the beginning of the lift phase, the oil cylinder of cam starts to pump oil. Because the oil pressure designed for starting the rear spring of the regulator is smaller than that for the valve spring, the oil will flow into the oil cylinder of regulator first, and the flow will continue until the plunger is stopped by the limit rod. Meanwhile, the valve will remain stationary, i.e. the leading angle of the valve will be reduced. As the cam continues to rotate, the oil pressure will further increase. Then, the driving force from the oil cylinder of valve will overcome the preload of the valve spring, and force open the valve. The degree of opening will gradually increase until the end of the lift phase.

The working order is reversed in the return phase. Because the oil pressure designed for starting the valve spring is greater than that of the rear spring of the regulator, the oil will flow back from the oil cylinder of valve, and the lift of the valve will gradually decrease. Once the valve falls back to a certain height, the seating snubber will be activated to ensure the stable seating of the valve. The cam will continue to rotate after the valve is seated. The oil in the oil cylinder of regulator will begin to flow back under the push of the rear spring of the regulator.

The flow back will not end until the cam returns to the base circle. Meanwhile, the valve will remain stationary, i.e. the lagging angle of the valve will be reduced.

Obviously, the continuous adjustment of valve phase can be achieved by properly adjusting the position of the limit rod in the regulator: after the adjustment, the operator can control the oil volume flowing into the oil cylinder of regulator, which in turn regulates the time and volume of the oil enters and exiting the oil cylinder of valve.

The crank angle-valve lift curves at the engine speed of 1,500 rpm (i.e. the camshaft speed of 750 rpm) were obtained in early tests on valve phase adjustment, and presented in Fig. 2, where A is the distance from the front end of the regulator to the limit rod, i.e. the adjustable range of the regulator. With the growth in the adjustable range, the leading angle, lagging angle and duration angle of the valve all exhibited a gradual decline, so did the lift of the valve.

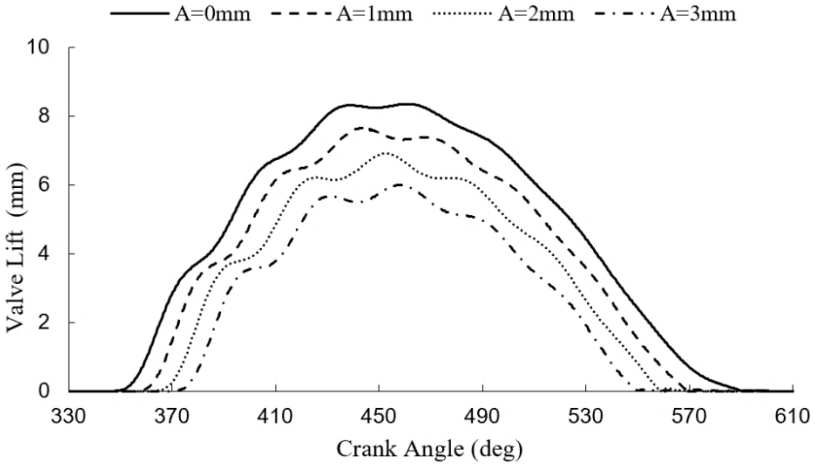


Figure 2: The crank angle-valve lift curves.

## 3. MATHEMATICAL MODELLING

Considering the structure of the target hydraulic VVT system and the influencing factors of valve motions, this section set up mathematical models for oil compressibility, pressure loss of pipeline, oil cylinder of cam, oil cylinder and buffer mechanism of the valve, oil cylinder of regulator, and the oil supply [26-28].

### 3.1 Mathematical model for oil compressibility

In hydraulic transmission, the oil is often simply treated as incompressible. In the hydraulic VVT system, however, the oil must be considered as a compressible fluid. Oil compressibility refers to the volume change of the oil under pressure. With the variation in oil pressure, the change of oil volume $\Delta V$ can be calculated by:

$$\Delta V = -\frac{\Delta P}{\beta} V \tag{1}$$

where, $V$ is the original volume of the oil; $\Delta P$ is the pressure change; $\beta$ is the effective bulk elastic modulus of the oil.

As shown in Eq. (1), the change of oil volume has a significant impact on the actual phase and lift of the valve, for the total oil volume $V$ in different parts of the system (including pipeline, oil cylinder of regulator, oil cylinder of cam and oil cylinder of valve) is far greater than the effective volume of the oil cylinder of cam. Therefore, the oil compressibility is non-negligible in the hydraulic VVT system.

### 3.2 Mathematical model for pipeline pressure loss

The pressure loss $\Delta p_\lambda$ of system pipeline is made up of the on-way pressure loss $\Delta p_{\lambda 1}$ and local pressure loss $\Delta p_{\lambda 2}$:

$$\Delta p_\lambda = \Delta p_{\lambda 1} + \Delta p_{\lambda 2} \tag{2}$$

The on-way pressure loss, induced by the internal and external frictions acting on the flowing oil, can be calculated by:

$$\Delta p_{\lambda 1} = k_\lambda \frac{l_g}{d_g} \cdot \frac{\rho v_y^2}{2} \tag{3}$$

where, $\rho$ is oil density; $d_g$ is pipeline diameter; $l_g$ is pipeline length; $v_y$ is flow velocity; $k_\lambda$ is the on-way resistance coefficient.

The local pressure loss is resulted from the collisions and fierce frictions between oil particles and between oil particle and pipeline wall, when local vortices are formed due to the sudden changes in flow direction and speed at the local obstacles (e.g. bend, joint, and sudden expansion/contraction of pipeline cross-section). The local pressure loss of the flowing oil can be calculated by:

$$\Delta p_{\lambda 2} = \xi \frac{\rho v_y^2}{2} \tag{4}$$

where, $\xi$ is the local resistance coefficient.

### 3.3 Mathematical model for the oil cylinder of cam

According to the continuity equation of fluids, the flow change $Q_t$ induced by plunger motions in the oil cylinder of cam can be described as:

$$Q_t = \frac{dx_t}{dt} \cdot \frac{\pi d_t^2}{4} \cdot \frac{\rho(p_t)}{\rho(0)} \tag{5}$$

where, $x_t = f(n)$ is the displacement of cam plunger, which is related to cam profile and cam speed; $d_t$ is the diameter of cam plunger; $p_t$ is the instantaneous pressure in the oil cylinder of cam; $\rho(p)$ is the oil density at the pressure $p$.

Through force analysis on cam plunger, the force balance equation can be obtained as:

$$F - f_{t0} - k_t x_t - p_t \frac{\pi d_{t1}^2}{4} - m_t \frac{d^2 x_t}{dt} = 0 \tag{6}$$

where, $F$ is the force between cam plunger and cam; $f_{t0}$ and $k_t$ are the preload and stiffness of the spring of cam plunger, respectively; $m_t$ is the mass of cam plunger.

### 3.4 Mathematical models for oil cylinder and buffer mechanism of the valve

There is a buffer mechanism at the bottom of the oil cylinder of valve. As shown in Fig. 3, the buffer mechanism consists of a check valve and a conical buffer device in the cylinder. The valve plunger is rigidly connected to the valve, so that the two components obey the same law of motions.

During the valve opening process, the oil in the main oil-way flows into the oil cylinder of valve via the check valve and the side oil-way, and drives the motions of valve plunger; the side oil-way has the same pressure as the main oil-way: ($p_q = p_z$).

During the valve closing process, the check valve is closed, and the oil in the oil cylinder of valve flows into the main oil-way through the side oil-way. As the valve approaches the seat, the flow area reduces between the conical plunger and the buffer hole, creating a conical

buffer segment. Then, the pressure in the oil cylinder of valve increases ($p_q < p_z$), forcing the valve plunger to slow down and ensuring the stable seating of the valve.

For the oil cylinder and buffer mechanism of the valve, different mathematical models should be constructed depending on the relative position between the valve and the conical buffer segment, because the buffer mechanism acts differently on the valve when the valve is outside or inside the conical buffer segment.

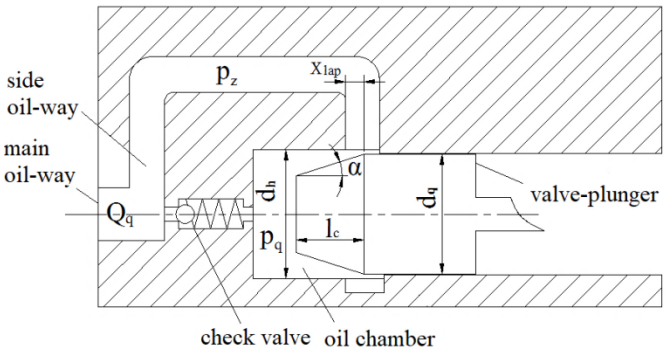


**Note**: $x_{lap}$ is the distance from the base of the cone to the buffer hole; $\alpha$ is the cone angle; $l_c$ is the cone length; $d_h$ is the inner diameter of the buffer hole; $d_q$ is the diameter of valve plunger; $d_a$ is the relative diameter of plunger.

Figure 3: Oil cylinder and buffer mechanism of the valve.

(1) Mathematical model when the valve is outside the conical buffer segment

From valve opening through vale closing to the start of buffering, the flow change $Q_q$ in the oil cylinder of valve can be defined as:

$$Q_q = \frac{dx_q}{dt} \cdot \frac{\pi d_q^{\,2}}{4} \cdot \frac{\rho(p_q)}{\rho(0)} \tag{7}$$

where, $x_q$ is the displacement of valve plunger, i.e. the valve displacement; $d_q$ is the diameter of valve plunger; $p_q$ is the instantaneous pressure in the oil cylinder of valve. During the said period, $p_q$ is equal to the side oil-way pressure: $p_q = p_z$.

Through force analysis on valve assembly, the force balance equation can be obtained as:

$$\frac{\pi d_q^2}{4} p_q - m_q \frac{d^2 x_q}{dt^2} - f_{q0} - k_q x_q = 0 \tag{8}$$

where, $m_q$ is the mass of valve assembly; $f_{q0}$ and $k_q$ are the preload and stiffness of the spring of valve assembly, respectively.

(2) Mathematical model when the valve is inside the conical buffer segment

The valve enters the conical buffer segment, when the cone flange of valve plunger moves close to the buffer hole at the bottom of the oil cylinder of valve. Then, the throttling of the check valve brings a pressure difference between the oil cylinder of valve and the side oil-way ($p_q \neq p_z$). Under the pressure difference, the pressure in the oil cylinder of valve will rise, forcing the valve plunger to slow down. Let $c_r = (d_h - d_q)/2$ be the minimum buffer gap and $A_q$ be the cross-sectional area of flow.

Then, the relationship between the flow in the oil cylinder of valve $Q_q$, the pressure in the oil cylinder of valve $p_q$ and the pressure in the side oil-way $p_z$ can be established as:

$$Q_q = \frac{dx_q}{dt} \cdot \frac{\pi d_q^{\,2}}{4} \cdot \frac{\rho(p_q)}{\rho(0)} = C_q A_q \sqrt{\frac{2 \cdot |p_q - p_z|}{\rho}} \tag{9}$$

Through force analysis on valve assembly, the force balance equation can be obtained as:

$$\frac{\pi(d_q^2 - d_a^2)}{4} p_z + \frac{\pi d_a^2}{4} p_q - m_q \frac{d^2 x_q}{dt^2} - f_{q0} - k_q x_q = 0 \tag{10}$$

### 3.5 Mathematical model for the oil cylinder of regulator

According to the continuity equation of fluids, the flow change $Q_a$ induced by plunger motions in the oil cylinder of regulator can be described as:

$$Q_a = \begin{cases} \frac{dx_a}{dt} \cdot \frac{\pi d_a^{\,2}}{4} \cdot \frac{\rho(p_a)}{\rho(0)} & x_a \neq A \\ 0 & x_a = A \end{cases} \tag{11}$$

where, $x_a$ is the displacement of regulator plunger; $d_a$ is the diameter of regulator plunger; $p_a$ is the instantaneous pressure in the oil cylinder of plunger; $A$ is the adjustable range of the plunger.

Next, the mass of regulator plunger $m_{a1}$ and the mass of regulator spring $m_{a2}$ were converted into a lumped mass $m_a = m_{a1} + \frac{1}{3} m_{a2}$ of the plunger assembly. Through force analysis on regulator plunger, the force balance equation can be obtained as:

$$\frac{\pi d_a^2}{4} p_a - m_a \frac{d^2 x_a}{dt^2} - f_{a0} - k_a x_a = 0 \tag{12}$$

where, $f_{a0}$ and $k_a$ are the preload and stiffness of plunger spring, respectively.

### 3.6 Mathematical model for the oil supply

The oil flow $Q_s$ from the oil supply to the VVT system via the check valve can be expressed as:

$$Q_s = \begin{cases} C_s A_s \sqrt{\frac{2 \times (p_i - p_s)}{\rho}} & , p_s \leq p_i \\ 0 & , p_s > p_i \end{cases} \tag{13}$$

where, $C_s$ is the flow coefficient; $A_s$ is the flow area of the check valve; $p_s$ is the instantaneous oil pressure of the system; $p_i$ is the initial oil pressure of the system.

## 4. SIMULATION MODEL

Based on the above mathematical models, a simulation model was established on AMESim to analyse and optimize the motion parameters of the hydraulic VVT system. As shown in Fig. 4, the simulation model includes a control subsystem (red), a hydraulic subsystem (blue and brown), and a mechanical subsystem (green). During the simulation, the cam drive was controlled by motor signals to adjust the engine speed. Besides, the adjustment of the limit rod was simulated by controlling the displacement of a mass block.

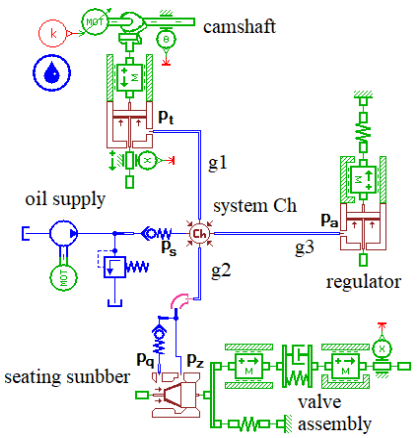


Figure 4: The AMESim simulation model for the target hydraulic VVT system.

The main parameters (Table I) of the AMESim simulation model were determined based on the physical parameters of the system and the mathematical models of the system.

Table I: The main parameters for AMESim simulation.

| Parameter | Value | Parameter | Value |
|---|---|---|---|
| $m_t$ (g) | 34 | $d_a$ (mm) | 10 |
| $m_q$ (g) | 110 | $d_q$ (mm) | 8 |
| $m_a$ (g) | 28 | $lg_1$ (mm) | 400 |
| $f_{t0}$ (N) | 10 | $lg_2$ (mm) | 400 |
| $f_{q0}$ (N) | 170 | $lg_3$ (mm) | 300 |
| $f_{a0}$ (N) | 80 | $V_{Ch}$ (mm$^3$) | 40,000 |
| $k_t$ (N/mm) | 1 | $\rho$ (g/mm$^3$) | $870\times10^{-6}$ |
| $k_q$ (N/mm) | 20 | $\xi$ (-) | 1.33 |
| $k_a$ (N/mm) | 3.69 | $\alpha$ (deg) | 15 |
| $d_t$ (mm) | 14 | $l_c$ (mm) | 3 |
| $d_q$ (mm) | 10 | $c_r$ (mm) | 0.06 |

## 5. ANALYSIS OF SIMULATION RESULTS

Fig. 5 presents the simulated crank angle-valve lift curves of the lift phase at the engine speed ($n$) of 1,000 rpm. With the growth in the adjustable range of the regulator, the leading angle, lagging angle and lift of the valve gradually decreased. The simulated trend is consistent with the valve adjustment function of the target system.

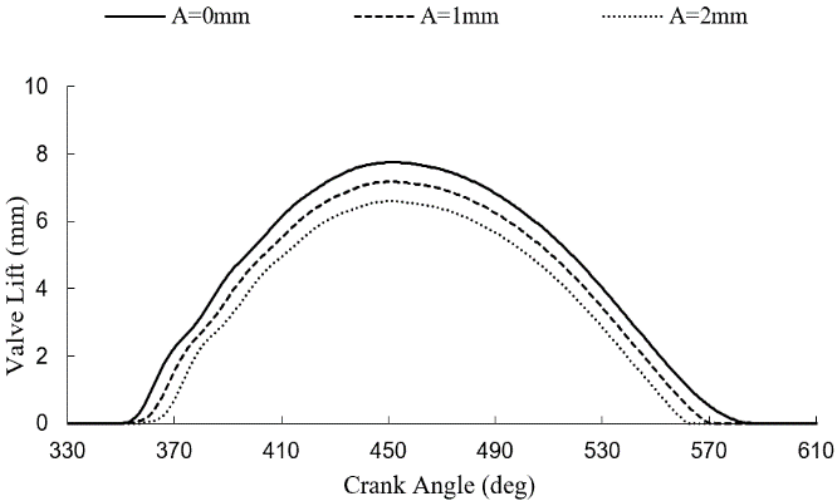


Figure 5: Simulated crank angle-valve lift curves of the lift phase at $n$ = 1,000 rpm.

Fig. 6 compares the simulated curves with the test curves. The comparison shows that the measured valve phases were basically the same as the simulated phases. The measured valve lift curves agreed well with the simulated curves: in the lift phase, the measured valve lift curves largely overlapped the simulated curves; in the return phase, the measured instantaneous lift curves were slightly below the simulated curves. Despite a slight difference between measured and simulated instantaneous oil pressures, the measured oil pressure curves had similar trends as the simulated curves. In addition, the crank angles and oil pressures corresponding to the peaks and valleys of the test curves were close to those of the simulated curves.

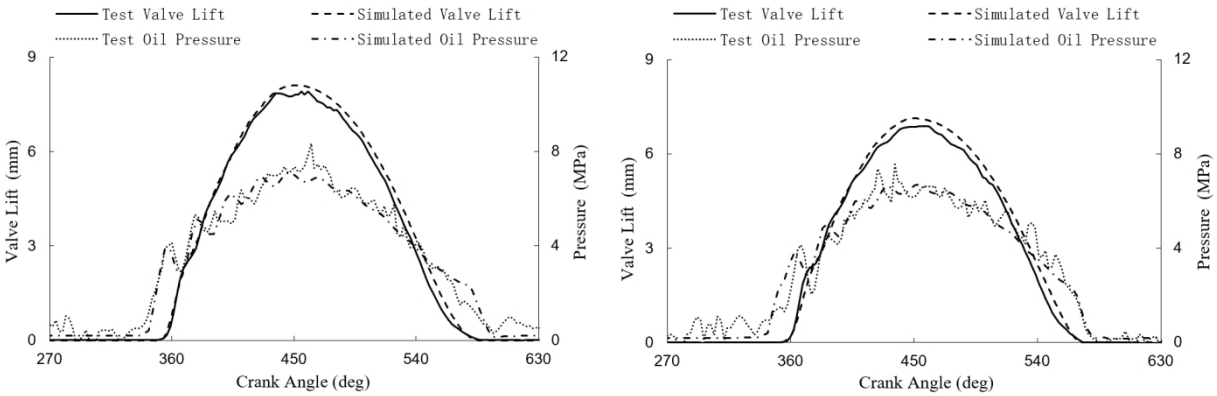


a) $n$ = 1,000 rpm, $A$ = 0 mm




b) $n$ = 1,000 rpm, $A$ = 1 mm

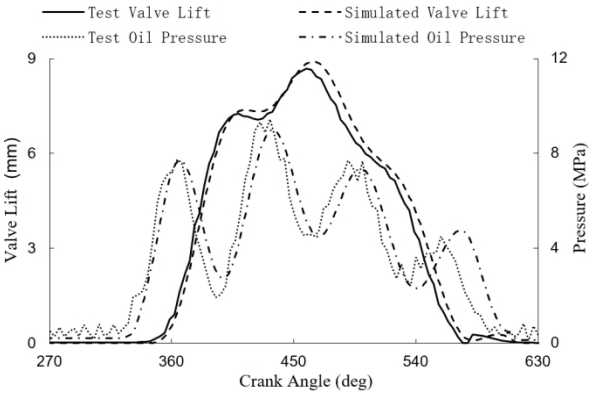


c) $n$ = 3,000 rpm, $A$ = 0 mm

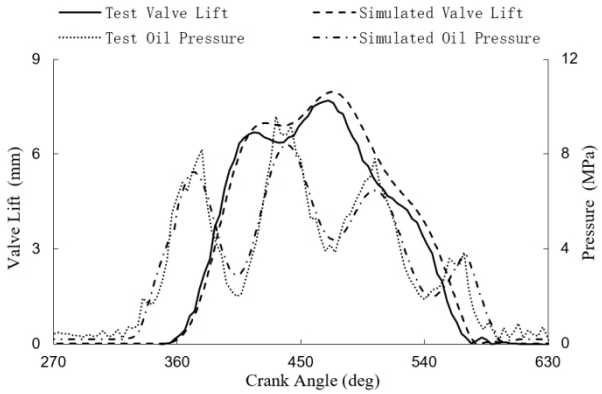


d) $n$ = 3,000 rpm, $A$ = 1 mm

Figure 6: Comparison between test curves and simulated curves.

The slight differences between simulated and test curves are attributable to the small oil leakage in the system, the machining errors of the parts, and the difference in oil pressure settings. (1) During the operation, it is inevitable for the system to have a certain amount of oil leakage. The leakage was not considered in our simulation model, because the leakage is very small, and the oil in the system is replenished before the next cycle. As a result, the measured lift is slightly smaller than the simulated lift in the return phase. (2) The cam profile and buffer cavity in our simulation are slightly different from those in the early tests, due to the machining errors of the components. (3) The oil pressure is constant in the simulation model, while that in the early tests has certain fluctuations.

To sum up, the simulated results are in good agreement with the test results, indicating that our simulation model is reliable and conducive to parameter analysis and optimization of valve motions.

## 6. CONCLUSIONS

This paper establishes mathematical models and a simulation model for a novel hydraulic VVT system, in the light of oil compressibility, pressure loss of pipeline, buffer mechanism of the valve, and regulator properties. Then, the target hydraulic VVT system was simulated on AMESim. The following conclusions were drawn through the simulation:

(1) The simulation model satisfies the requirements on the performance analysis of the hydraulic VVT system, and can effectively simulate the motions, kinetic parameters, and hydraulic parameters of the target system.

(2) The comparison between simulated results and early test results shows that: The measured valve lift curves agreed well with the simulated curves. Despite a slight difference

between measured and simulated instantaneous oil pressures, the measured oil pressure curves had similar trends as the simulated curves. In addition, the crank angles and oil pressures corresponding to the peaks and valleys of the test curves were close to those of the simulated curves.

(3) The slight differences between simulated and test curves are attributable to the small oil leakage in the system, the machining errors of the parts, and the difference in oil pressure settings.

(4) The simulated results are in good agreement with the test results, indicating that our simulation model is reliable and conducive to parameter analysis and optimization of valve motions.

## ACKNOWLEDGEMENTS

This work was supported by Guiyang University Research Fund [GYU-KJZ (2019-2020) PT08-03], Guizhou Provincial Education Department Talent Growth Project [KY (2019)087] and Guizhou Science and Technology Foundation [2020]1Y226.

## REFERENCES

[1] Schechter, M. M.; Levin, M. B. (1996). *Camless Engine*, SAE Technical Paper 960581, 15 pages, Society of Automotive Engineers, doi:10.4271/960581

[2] Damasceno, L. I. R.; Gallo, W. L. R. (2013). Variable valve timing and its effects on performance of a spark-ignition engine, *Proceedings of the 22nd SAE Brasil International Congress and Display*, Paper 2013-36-0318, 12 pages, doi:10.4271/2013-36-0318

[3] Cairns, A.; Zhao, H.; Todd, A.; Aleiferis, P. (2013). A study of mechanical variable valve operation with gasoline-alcohol fuels in a spark ignition engine, *Fuel*, Vol. 106, 802-813, doi:10.1016/j.fuel.2012.10.041

[4] Vos, K. R.; Shaver, G. M.; Joshi, M. C.; McCarthy Jr., J. (2019). Implementing variable valve actuation on a diesel engine at high-speed idle operation for improved aftertreatment warm-up, *International Journal of Engine Research*, 13 pages, in press, doi:10.1177/1468087419880639

[5] Zou, P.; Liu, J.; Zhou, X.; Chen, Z.; Luo, B.; Shen, D.; Duan, X.; Fu, J. (2020). Effect of a novel mechanical CVVL system on economic performance of a turbocharged spark-ignition engine fuelled with gasoline and ethanol blend, *Fuel*, Vol. 263, Paper 116697, 14 pages, doi:10.1016/j.fuel.2019.116697

[6] Moriya, Y.; Watanabe, A.; Uda, H.; Kawamura, H.; Yoshioka, M.; Adachi, M. (1996). *A newly developed intelligent variable valve timing system – continuously controlled cam phasing as applied to a new 3 liter inline 6 engine*, SAE Technical Paper 960579, 9 pages, Society of Automotive Engineers, doi:10.4271/960579

[7] Jung, H. H.; Stein, R. A.; Leone, T. G. (2004). *Comparison of dual retard VCT to continuously variable event valvetrain*, SAE Technical Paper 2004-01-1268, 13 pages, Society of Automotive Engineers, doi:10.4271/2004-01-1268

[8] Benedikt, K.; Drexler, G.; Eder, T.; Eisenkoelbl, M.; Luttermann, C.; Schleusener, M. (2005). Further development of BMW's fully-variable valve control system Valvetronic, *MTZ Worldwide*, Vol. 66, No. 9, 10-13, doi:10.1007/BF03227780

[9] Hosaka, T.; Hamazaki, M. (1991). *Development of the variable valve timing and lift (VTEC) engine for the Honda NSX*, SAE Technical Paper 910008, 7 pages, Society of Automotive Engineers, doi:10.4271/910008

[10] Wurms, R.; Dengler, S.; Budack, R.; Mendl, G.; Dicke, T.; Eiser, A. (2006). Audi valvelift system – a new innovative valve train system designed by Audi, *Proceedings of the 15th Aachen Colloquium*, 1069-1093

[11] Bharath, A. N.; Yang, Y.; Reitz, R. D.; Rutland, C. (2015). *Comparison of variable valve actuation, cylinder deactivation and injection strategies for low-load RCCI operation of a light duty engine*, SAE Technical Paper 2015-01-0843, 12 pages, Society of Automotive Engineers, doi:10.4271/2015-01-0843

[12] Xu, Y.; Wang, Z.; Chen, J. (2016). Hydraulic variable valve system for improving the performance of internal combustion engine, *Scientific Bulletin of National Mining University*, Vol. 2016, No. 1, 53-58
[13] Pournazeri, M.; Khajepour, A.; Huang, Y. (2017). Development of a new fully flexible hydraulic variable valve actuation system for engines using rotary spool valves, *Mechatronics*, Vol. 46, 1-20, doi:10.1016/j.mechatronics.2017.06.010
[14] Pournazeri, M.; Khajepour, A.; Huang, Y. (2018). Improving energy efficiency and robustness of a novel variable valve actuation system for engines, *Mechatronics*, Vol. 50, 121-133, doi:10.1016/j.mechatronics.2018.02.002
[15] Mehrabi, S.; Kheradmand, S.; Farivar, O. R. (2018). Numerical simulation of thermal and hydraulic performance of a micro plate-pin fin heat sink, *International Journal of Heat and Technology*, Vol. 36, No. 3, 883-894, doi:10.18280/ijht.360315
[16] Pournazeri, M.; Khajepour, A. (2016). Precise lift control in a new variable valve actuation system using discrete-time sliding mode control, *Mechanism and Machine Theory*, Vol. 99, 217-235, doi:10.1016/j.mechmachtheory.2016.01.007
[17] Wong, P. K.; Tam, L. M.; Li, K. (2008). Modelling and simulation of a dual-mode electrohydraulic fully variable valve train for four-stroke engines, *International Journal of Automotive Technology*, Vol. 9, No. 5, 509-521, doi:10.1007/s12239-008-0061-2
[18] Wong, P.; Mok, K. (2008). *Design and modelling of a novel electromechanical fully variable valve system*, SAE Technical Paper 2008-01-1733, 12 pages, Society of Automotive Engineers, doi:10.4271/2008-01-1733
[19] Xie, Z.; Zhang, J.; Chang, Y. (2014). *Study on intake performance of unthrottled SI engine with fully variable hydraulic valve actuating system*, SAE Technical Paper 2014-01-2872, 11 pages, Society of Automotive Engineers, doi:10.4271/2014-01-2872
[20] Herranen, M.; Huhtala, K.; Vilenius, M.; Liljenfeldt, G. (2007). *The electro-hydraulic valve actuation (EHVA) for medium speed diesel engines – development steps with simulations and measurements*, SAE Technical Paper 2007-01-1289, 10 pages, Society of Automotive Engineers, doi:10.4271/2007-01-1289
[21] Zhou, X. J.; Chen, Z.; Zou, P.; Liu, J. P.; Duan, X. B.; Li, Q. Y.; Shen, D. Z. (2020). Kinematics analysis and design method of a new mechanical CVVL system with self-regulation of the valve timing, *Mechanism and Machine Theory*, Vol. 143, Paper 103624, 22 pages, doi:10.1016/j.mechmachtheory.2019.103624
[22] Wang, Y.; Long, W.; Cui, J.; Tian, H.; Meng, X.; Wang, X.; Xu, D. (2020). Development of a variable mode valve actuation system for a heavy-duty engine, *Proceedings of the Institution of Mechanical Engineers, Part D: Journal of Automobile Engineering*, 16 pages, in press, doi:10.1177/0954407020901659
[23] Gillella, P.; Sun, Z. (2010). Design, modelling, and control of a camless valve actuation system with internal feedback, *IEEE/ASME Transactions on Mechatronics*, Vol. 16, No. 3, 527-539, doi:10.1109/TMECH.2010.2045656
[24] Menni, Y.; Chamkha, A. J.; Lorenzini, G.; Benyoucef, B. (2019). Computational fluid dynamics based numerical simulation of thermal and thermo-hydraulic performance of a solar air heater channel having various ribs on absorber plates, *Mathematical Modelling of Engineering Problems*, No. 6, No. 2, 170-174, doi:10.18280/mmep.060203
[25] Mercorelli, P.; Werner, N. (2016). An adaptive resonance regulator for an actuator using periodic signals in camless engine systems, *IFAC-PapersOnLine*, Vol. 49, No. 14, 176-181, doi:10.1016/j.ifacol.2016.07.1005
[26] Kim, B. S.; Kim, T. G. (2019). Cooperation of simulation and data model for performance analysis of complex systems, *International Journal of Simulation Modelling*, Vol. 18, No. 4, 608-619, doi:10.2507/IJSIMM18(4)491
[27] Szydłowski, T.; Smoczyński, M. (2013). Simulation research of the hydraulic drive for valves of internal combustion engine, *Journal of KONES*, Vol. 20, No. 2, 385-391
[28] Edler, J.; Tic, V.; Lovrec, D. (2019). 1-D simulation model of a progressive flow controller for hydrostatic bearings, *International Journal of Simulation Modelling*, Vol. 18, No. 2, 267-278, doi:10.2507/IJSIMM18(2)472